Available online at www.sciencedirect.com
SCIENCE DIRECT
Journal of Magnetic Resonance 180 (2006) 170–177
JMR Journal of Magnetic Resonance
www.elsevier.com/locate/jmr

Satellite transitions in natural abundance solid-state ^{33}S MAS NMR of alums—Sign change with zero-crossing of C_Q in a variable temperature study

Hans J. Jakobsen *, Anders R. Hove, Henrik Bildsøe, Jørgen Skibsted

Instrument Center for Solid-State NMR Spectroscopy, Department of Chemistry, University of Aarhus, DK-8000 Aarhus C, Denmark

Received 15 December 2005; revised 3 February 2006
Available online 21 February 2006

Abstract

Experiences obtained from recent improvements in the performance of solid-state ^{14}N MAS NMR spectroscopy have been used in a natural abundance ^{33}S MAS NMR investigation of the satellite transitions for this interesting spin $I = 3/2$ isotope. This study reports the first observation of manifolds of spinning sidebands for these transitions in ^{33}S MAS NMR as observed for the two alums $XAl(SO_4)_2{\cdot}12H_2O$ with $X = NH_4$ and K. For the NH_4-alum a variable temperature ^{33}S MAS NMR study, employing the satellite transitions, shows that the ^{33}S quadrupole coupling constant (C_Q) exhibits a linear temperature dependence (in the range -35 °C to 70 °C) with a temperature gradient of 3.1 kHz/°C and undergoes a sign change with zero-crossing for C_Q at 4 °C (277 K). For the isostructural K-alum a quite similar increase in the magnitude of C_Q with increasing temperature is observed, and with a temperature gradient of 2.3 kHz/°C. Finally, for optimization purposes, a study on the effect of the applied pulse widths at constant rf field strength on the intensity and variation in second-order quadrupolar lineshape for the central ($1/2 \leftrightarrow -1/2$) transition of the K-alum has been performed.

Keywords: ^{33}S MAS NMR; Satellite transitions; Alums; Variable-temperature NMR; Sign change of C_Q; Simulations

1. Introduction

Nitrogen and sulfur range among the most important light elements in the chemistry of inorganic materials but also of many organic and biomolecules. However, from a NMR point of view the two natural abundant spin isotopes ^{14}N (99.63%) and ^{33}S (0.76%) have found limited applications for obvious reasons. These limitations apply first of all to studies in the solid-state whereas more work has been performed on compounds in solution, in particular for ^{14}N [1].

Natural abundance ^{14}N and ^{33}S NMR in solids are considered two extremely difficult experimental techniques because both isotopes are low-γ quadrupolar nuclei with spin $I = 1$ and $I = 3/2$, respectively. Considering the absolute receptivities for ^{14}N and ^{33}S relative to ^{13}C at natural abundance (2.1499 and 0.0194, respectively), the factor of 110 higher receptivity for ^{14}N relative to ^{33}S would seem to indicate a much higher sensitivity for ^{14}N as is also observed in liquid-state NMR studies. However, in solid-state NMR, the experimental difficulties for ^{14}N and ^{33}S become more similar for different reasons. The main reason which makes solid-state ^{14}N NMR a low-sensitivity technique is because its integer spin ($I = 1$) precludes the detection of a central transition as is usually observed for half-integer quadrupolar nuclei. This restricts ^{14}N observation to the detection of the ($1 \leftrightarrow 0$) and ($0 \leftrightarrow -1$) transitions and thereby makes the sensitivity extremely dependent on the width of these transitions, i.e., on the first-order quadrupolar broadening, directly proportional to the magnitude of the ^{14}N quadrupolar coupling constant. On the other hand, in solid-state ^{33}S NMR the spin $I = 3/2$ for ^{33}S allows observation of the central

* Corresponding author. Fax: +45 8619 6199.
E-mail address: hja@chem.au.dk (H.J. Jakobsen).

1090-7807/$ - see front matter © 2006 Elsevier Inc. All rights reserved.
doi:10.1016/j.jmr.2006.02.006

$(1/2 \leftrightarrow -1/2)$ transition, a transition not broadened by the first-order quadrupole interaction but only to second order. Since the second-order quadrupolar broadening of the central transition is inversely proportional to the magnetic field strength (in contrast to the broadening by the first-order interaction), the sensitivity of the ^{33}S central transition resonance clearly benefits from applying the highest possible field strength. This was recently demonstrated experimentally in a high-field ^{33}S MAS NMR study of the ^{33}S central transition for some inorganic sulfates [2], for example by comparison with results obtained about two decades ago at lower magnetic field strength [3].

In recent years, we have put great efforts into improving the experimental strategies for the observation of high-quality ^{14}N MAS NMR spectra which allow simulation and/or optimization of ^{14}N spinning sidebands (ssb) patterns covering a spectral width up to about 2 MHz [4–10]. Thereby it has been possible to extract precise values for the ^{14}N quadrupole coupling constants (C_Q) as large as 1.2–1.5 MHz [8,10] along with the corresponding asymmetry parameters (η_Q) from these spectra. In particular, we note that by coupling the precise experimental ^{14}N parameters (C_Q, η_Q), as for example determined for $CsNO_3$ [9], with density functional theory (DFT) calculations has allowed refinement of its fractional atomic coordinates determined by single-crystal XRD [9], a strategy which may have great potential to ^{33}S C_Q, η_Q parameters. Because the ^{14}N and ^{33}S quadrupolar nuclei are neighbors in the low-frequency end of the NMR-frequency table, we have taken full advantage of all experimental experiences gained from our ^{14}N MAS NMR studies in the present investigation on a precise determination of ^{33}S quadrupole coupling parameters from natural-abundance ^{33}S MAS NMR.

In this communication, we present the first experimental observation of ^{33}S spinning sideband (ssb) patterns for the satellite transitions determined from natural-abundance ^{33}S MAS NMR spectra. These have proven useful with respect to extracting ^{33}S quadrupole coupling parameters (C_Q, η_Q) of high precision. This is illustrated by observation of the ssb pattern for the sulfate ions of the two alums $NH_4Al(SO_4)_2{\cdot}12H_2O$ and $KAl(SO_4)_2{\cdot}12H_2O$, i.e., samples which are included in the recent high-field ^{33}S MAS NMR study of the central transition for some inorganic sulfates [2]. In that study the linewidth observed for the central transition of $NH_4Al(SO_4)_2{\cdot}12H_2O$ is too narrow to allow determination of the ^{33}S C_Q, η_Q parameters from the second-order quadrupole broadening. In addition, no ssb pattern seems apparent from the published spectra of this alum or from the spectra for any of the other inorganic sulfates which would allow such a determination. The present study shows that it has not only been possible to observe ^{33}S ssb patterns for $NH_4Al(SO_4)_2{\cdot}12H_2O$ but also to detect a linear temperature dependence and a sign change with zero-crossing for C_Q at +4 °C (277 K) for this alum in the course of a variable temperature study. To the best of our knowledge, this is the first experimentally observed zero-crossing for a quadrupole coupling constant, at least observed by solid-state NMR techniques. Finally, the observation of a ssb pattern for the alum $KAl(SO_4)_2{\cdot}12H_2O$ supports conclusions reached from earlier studies of other half-integer nuclei [11,12] that C_Q, η_Q parameters for quadrupolar nuclei may be determined with higher precision employing the ssbs for the satellite transitions as compared to the second-order lineshape for the central transition.

2. Experimental

The two alums $XAl(SO_4)_2{\cdot}12H_2O$, with $X = NH_4$ and K, are both commercially available and were used without further purification.

^{33}S MAS NMR experiments were performed at 46.01 MHz on a Varian *Unity* INOVA-600 spectrometer equipped with a 14.1 T widebore magnet. Two probes, a Varian/Chemagnetics broadband 7.5 mm T3 CP/MAS probe and a homemade 5 mm variable-temperature (VT) CP/MAS probe, were used for the room-temperature and variable-temperature experiments, respectively. The rotor spinning frequencies (ν_r) for the 7.5 mm probe were in the range from 1500 to 6000 Hz, dependent on the magnitude of the ^{33}S quadrupole coupling constants, and were stabilized to $\leqslant$1 Hz for both probes using Varian/Chemagnetics MAS-speed controllers. The magic angle of $\theta = 54.736°$ was adjusted to the highest possible precision ($<\pm 0.005°$) by performing ^{14}N MAS NMR (43.34 MHz) on a sample of $(CH_3)_4NI$ or $NH_4H_2PO_4$ (i.e., by narrowing the centerband linewidth from a doublet at off-angle conditions to a narrow singlet at magic-angle setting [6]) or using a sample of $Pb(NO_3)_2$ [7]. The idea of using ^{14}N MAS NMR for the magic-angle adjustment is that it allows tuning back and forth between ^{33}S and ^{14}N without making any hardware changes (e.g., tuning tubes/wands) to the probes outside the magnet. The variable-temperature ^{33}S MAS experiments were performed in the temperature range −35 to +70 °C using the homemade 5 mm VT CP/MAS probe ($\nu_r = 6000$–10,000 Hz) coupled to a XRII851 Air-Jet sample cooling/heating system (FTS Systems, Stone Ridge, NY 12484) supplying the VT air to a combination of the double air-bearing and jets directed onto the rotating sample. In this manner the temperature gradient across the sample has been determined to be $\leqslant$1 °C for the spinning frequencies and temperature range employed in this research. The actual sample temperatures and temperature gradients were calibrated using ^{207}Pb MAS NMR of an external sample of $Pb(NO_3)_2$ under identical experimental conditions.

For both probes acquisition of the ^{33}S MAS NMR spectra employed single-pulse excitation, a flip angle generally about 55° (i.e., $\tau_p = 3$–4 μs for τ_p^{90}(liquid) = 5.0–6.5 μs), a spectral width varying from 0.3 to 1.0 MHz, and relaxation delays varying from 0.5 to 2 s. The pulse-width calibration employed an external sample of 1.0 M aqueous Cs_2SO_4 which was also used as a secondary ^{33}S chemical shift ref-

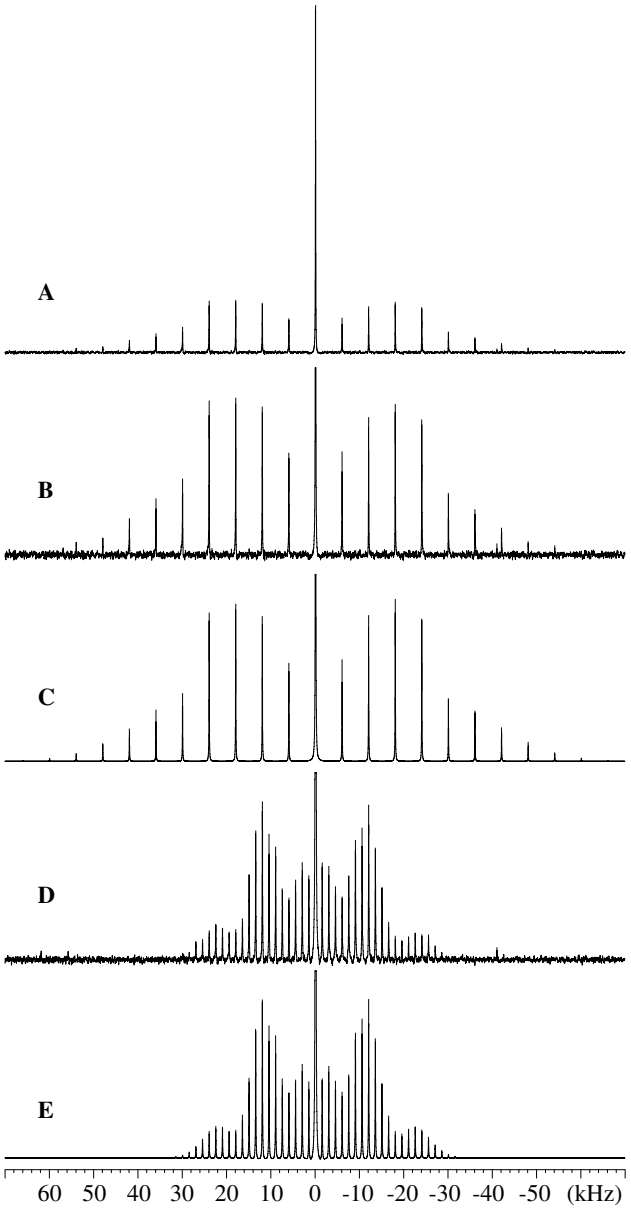

Fig. 1. Experimental (natural abundance) and simulated ^{33}S MAS NMR spectra (46.04 MHz at 14.1 T) of $NH_4Al(SO_4)_2{\cdot}12H_2O$ recorded at ambient temperature for two different spinning frequencies, ν_r. The experimental spectrum (A) employed $\nu_r = 6000$ Hz, 26000 scans, and has a vertical expansion which shows the actual relative heights between the central transition and the ssbs of the satellite transitions. In (B) the experimental spectrum is displayed with a vertical expansion larger by a factor 3 than that in (A) and with a cut-off height at 18% for the height of the central transition. The experimental spectrum (D) used $\nu_r = 1500$ Hz, 125,000 scans, and a cut-off height at 10% of the central transition. The simulated spectrum (C) used the optimized parameters $C_Q = 106.1$ kHz and $\eta_Q = 0.05$ (Table 1) and a small value, $\delta_\sigma = 10$ ppm and $\eta_\sigma = 0$, for the chemical shift anisotropy in order to fine tune the slight asymmetry observed for the ssb intensities relative to the center of the spectrum. The simulated spectrum in (E) employed the (optimized) parameters $C_Q = 56.5$ kHz and $\eta_Q = 0.11$ (Table 1) and with $\delta_\sigma = 5$ ppm, $\eta_\sigma = 0$ for the chemical shift anisotropy to account for the slight asymmetry observed for the ssb intensities. The chemical shift scale is shown in kHz and is relative to a 1.0 M solution of Cs_2SO_4 (see Section 2).

erence (333 ppm relative to CS_2). ^{1}H decoupling during acquisition was applied to the spectra recorded for spinning frequencies $\nu_r \leqslant 2000$ Hz in order to reduce the increase in linebroadening caused by the residual ^{33}S–^{1}H dipolar coupling at low-speed MAS (averaged at high-speed MAS). The ^{1}H decoupling was performed using two homemade in-series 600 MHz traps in the observe line from the preamp to the probe (as opposed to a standard low-pass filter) [10]. The reason is that the use of low-pass/band-pass filters in the observe line at the low frequencies of 43 and 46 MHz (14.1 T) for ^{14}N and ^{33}S, respectively, highly affects the rf bandwidth as recently demonstrated for ^{14}N MAS NMR [8].

All spectra were analyzed by simulation/iterative fitting on a Sun Microsystem Ultra-5 workstation using the STARS solid-state NMR software package developed in our laboratory [13] and incorporated into the Varian VNMR software. The quadrupolar coupling parameters employed in the simulations using STARS are related to the principal elements of the electric-field gradient tensor (**V**) by:

$$C_Q = \frac{eQV_{zz}}{h}, \tag{1}$$

$$\eta_Q = \frac{V_{yy} - V_{xx}}{V_{zz}}, \tag{2}$$

where the principal tensor elements are defined by $|V_{zz}| \geqslant |V_{xx}| \geqslant |V_{yy}|$.

Because of the negligibly small ^{33}S chemical shift anisotropy (CSA) apparent from the ambient temperature ^{33}S MAS spectra of the alum (sulfate ion) in Fig. 1, i.e., $\delta_\sigma(^{33}\mathrm{S}) = |\delta_{zz} - \delta_{iso}| \leqslant 10$ ppm (or the span of the chemical shift tensor $|\Omega| = |\delta_{zz} - \delta_{xx}| \leqslant 15$ ppm), the effect of the ^{33}S CSA on the appearance of the variable temperature ^{33}S MAS NMR spectra can be neglected and has generally not been considered in the analysis of these spectra.

3. Results and discussion

The natural-abundance ^{33}S MAS NMR spectrum of $NH_4Al(SO_4)_2{\cdot}12H_2O$ recorded at an "apparent" ambient temperature of 22 °C for $\nu_r = 6000$ Hz displays a distinct first-order ssb pattern for the two satellite transitions ($+3/2 \leftrightarrow +1/2$ and $-3/2 \leftrightarrow -1/2$) in addition to a narrow central transition ($+1/2 \leftrightarrow -1/2$) as shown in Fig. 1A. Thus, the ^{33}S MAS spectrum in Fig. 1A (vertical expansion in Fig. 1B) allows determination of the C_Q, η_Q parameters by iterative fitting of the simulated to the experimental intensities of the ssbs using STARS. Thereby, the values $C_Q = 106.1$ kHz and $\eta_Q = 0.05$ (Table 1) are obtained and the simulated spectrum corresponding to these parameters is presented in Fig. 1C. It is noted that an upper limit for C_Q of 530 kHz in $NH_4Al(SO_4)_2{\cdot}12H_2O$ has been reported in the early solid-state ^{33}S NMR study using static conditions [3], while C_Q could not be determined from the narrow central transition in the recent ^{33}S MAS NMR study (i.e., quote: "C_Q is very small") [2].

Table 1
Temperature dependence of ^{33}S quadrupolar coupling parameters (C_Q, η_Q) and isotropic chemical shifts (δ_{iso}) for the two alums $XAl(SO_4)_2{\cdot}12H_2O$, X = NH_4 and K[a]

Compound	Experimental	ν_r (kHz)	Temperature[b](°C)	C_Q (kHz)	η_Q	δ_{iso}[c] (ppm)
$NH_4Al(SO_4)_2{\cdot}12H_2O$	Ambient	6.0[d]	(38)	106.1	0.05	330.4
—	Ambient	1.5[d]	(23)	56.5	0.11	330.3
$NH_4Al(SO_4)_2{\cdot}12H_2O$	VT[e]	6.0	69	200.4	0.06	330.8
—	—	6.0	62	178.7	0.03	330.6
—	—	6.0	51	143.1	0.06	330.5
—	—	6.0	40	109.5	0.08	330.4
—	—	6.0	25	65.9	0.17	330.3
—	—	3.0	21	55.2	0.12	330.3
—	—	6.0	17	43.2	0.29	330.2
—	—	3.0	14	33.3	0.25	330.2
—	—	3.0	7	6.3	0.27	330.1
—	—	3.0	−2	−19.4	0.09	330.0
—	—	3.0	−7	−44.8	0.11	329.9
—	—	3.0	−22	−84.4	0.07	329.7
—	—	3.0	−36	−121.1	0.05	329.7
$KAl(SO_4)_2{\cdot}12H_2O$	Ambient	6.0[d]	(37)	638.4	0.04	331.5
—	Ambient	10.0[e]	(31)	626	0.04	331.7
$KAl(SO_4)_2{\cdot}12H_2O$	VT[e]	6.0	55	680	0.00	332.2
—	—	6.0	38	641	0.00	332.1
—	—	6.0	5	566	0.01	331.6
—	—	6.0	−15	521	0.01	331.4
—	—	6.0	−46	452	0.03	331.2

[a] The error limits for C_Q, η_Q, and δ_{iso} are better than ±3 (kHz), ±0.05, and ±0.2 ppm. In the temperature range 25 to −20 °C, the error limit for η_Q in $NH_4Al(SO_4)_2{\cdot}12H_2O$ may be slightly larger because of the reduced number of ssbs observed. Although the sign for C_Q is unknown, a positive sign has been assigned for C_Q above 4 °C in this table.
[b] The temperature has been calibrated to within ±1 °C using ^{207}Pb VT MAS on $Pb(NO_3)_2$. The temperatures in parentheses are calculated from the C_Q values using Eq. (3) for $NH_4Al(SO_4)_2{\cdot}12H_2O$ and Eq. (5) for $KAl(SO_4)_2{\cdot}12H_2O$ (see text).
[c] The δ_{iso} values include corrections for the second-order quadrupolar shifts which at 14.1 T are in the range −2.4 to −5.5 ppm for the $KAl(SO_4)_2{\cdot}12H_2O$ data and in the range 0 to −0.5 ppm for $NH_4Al(SO_4)_2{\cdot}12H_2O$.
[d] Using a Varian/Chemagnetics 7.5 mm T3 CP/MAS probe.
[e] Using a homemade 5 mm VT CP/MAS probe.

Most surprisingly, when recording the ambient-temperature ^{33}S MAS NMR spectrum of $NH_4Al(SO_4)_2{\cdot}12H_2O$ at the reduced spinning frequency of $\nu_r = 1500$ Hz, with the purpose of introducing more detailed features into the envelope of ssbs for the satellite transitions, a shrinkage in the width of these transitions is observed as illustrated by the experimental spectrum in Fig. 1D. Optimization of simulated spectra to the spectrum in Fig. 1d results in the simulation shown in Fig. 1E and the quadrupole coupling parameters $C_Q = 56.5$ kHz and $\eta_Q = 0.11$ (Table 1), thereby reflecting the reduced width of the spectrum. The reduced frictional heating at the lower spinning frequency, a phenomenon reported earlier from our laboratory [5,14], would seem to indicate a fairly strong temperature dependence for C_Q in $NH_4Al(SO_4)_2{\cdot}12H_2O$, i.e., the magnitude of C_Q increases with an increase in temperature. It is noted that because the sign of C_Q at ambient temperature is unknown, we use the term 'magnitude of C_Q' throughout this paper, i.e., $|C_Q|$ corresponding to a positive C_Q at ambient temperature. To investigate this hypothesis, a series of VT ^{33}S MAS NMR experiments, employing a fixed spinning frequency of 6000 Hz above ambient temperature and 3000 Hz below ambient, have been performed in the temperature range −35 to +70 °C (238–343 K). Increasing the temperature from ambient to 70 °C, a linear increase in the magnitude for C_Q from ~60 to ~200 kHz is observed (Table 1), i.e., an increase of ~3 kHz per degree. This would indicate that (i) by cooling the sample C_Q should vanish (zero-cross) just above 0 °C, and that (ii) assuming a continuous linear temperature dependence a sign change should occur for C_Q values below 0 °C. That both of these predictions are met, can be seen from the series of selected VT ^{33}S MAS NMR spectra, covering the VT range studied and displayed in Fig. 2. The corresponding set of spectral parameters (C_Q, η_Q, and δ_{iso}) extracted from these spectra are summarized in Table 1 along with the data determined from the VT spectra not shown in Fig. 2. These data reveal a linear correlation between C_Q and temperature as depicted in Fig. 3 and regression analysis gives

$$C_Q\ (\text{kHz}) = 3.114 \times T(^\circ\text{C}) - 13.6 \quad (3)$$

with a correlation coefficient $R = 0.9993$. From this graph we observe that the sign change (i.e., the zero-crossing) for C_Q occurs at a temperature of 4 °C (277 K) and with a temperature gradient $dC_Q/dT = 3.1$ kHz/°C. Also, from the correlation in Eq. (3) we deduce from the C_Q values

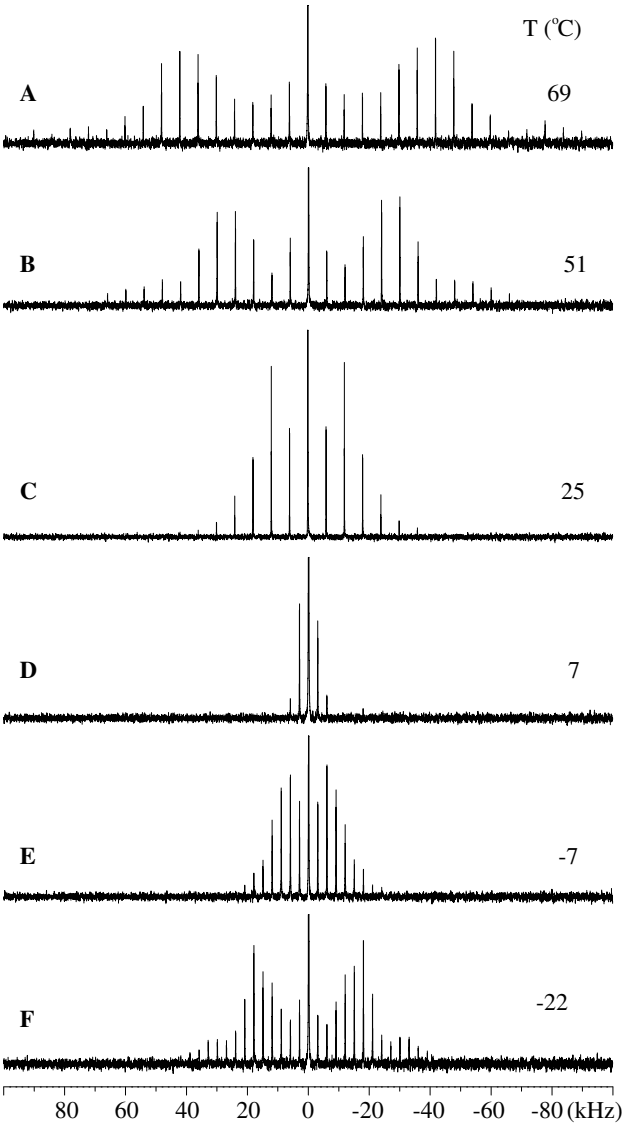

Fig. 2. Selected experimental variable-temperature (VT) ^{33}S MAS NMR spectra of $NH_4Al(SO_4)_2{\cdot}12H_2O$ showing the temperature dependence observed for the manifold of ssbs for the ^{33}S ($\pm 3/2 \leftrightarrow \pm 1/2$) satellite transitions in the temperature range from 69 °C to −22 °C and illustrating the sign change for C_Q. Spectra recorded at and above ambient temperature used $\nu_r = 6000$ Hz while the spectra obtained at and below ambient used $\nu_r = 3000$ Hz in order to introduce enhanced detailed features into the envelope of ssbs illustrating the zero-crossing for C_Q. Spectra acquired in the temperature range from 50 to 70 °C employed between 280,000 and 430,000 scans while the spectra taken below 50 °C all used ~145,000 (±5%) scans. The individual spectra are plotted employing a vertical scaling factor (vsf) relative to that used for the spectrum in (C). The vsf and sample temperature (T °C) for the individual spectra are indicated in the following. (A) $T = 69$ °C and vsf = 3.0. (B) $T = 51$ °C and vsf = 2.0. (C) $T = 25$ °C and vsf = 1.0. (D) $T = 7$ °C and vsf = 1.5. (E) $T = -7$ °C and vsf = 1.5. (F) $T = -22$ °C and vsf = 2.0. The spectral parameters (C_Q, η_Q, and δ_{iso}) determined from the VT ^{33}S MAS NMR spectra are summarized in Table 1. The chemical shift scale is shown in kHz and is relative to a 1.0 M solution of Cs_2SO_4 (see Section 2).

(Table 1) that the temperatures of the sample corresponding to the experimental spectra in Figs. 1A and B ($\nu_r = 6.0$ kHz) and Fig. 1D ($\nu_r = 1.5$ kHz) are 38 and 23 °C, respectively. The temperature of 38 °C determined

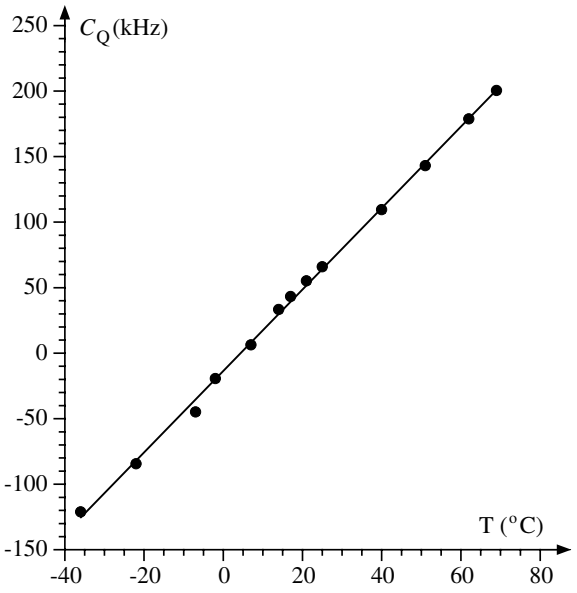

Fig. 3. Regression analysis of the C_Q versus T (°C) data in Table 1 for the temperature dependence of C_Q in $NH_4Al(SO_4)_2{\cdot}12H_2O$. The result shows an excellent linear correlation, expressed by Eq. (3), and a sign change for C_Q at 4 °C.

for the sample spinning at $\nu_r = 6.0$ kHz using ambient temperature air (21 °C) is in excellent agreement with the phase transition ($\alpha \leftrightarrow \beta$) at 37 °C for NH_4NO_3, also observed employing ^{14}N MAS NMR for $\nu_r = 6$–7 kHz using ambient temperature air under the same experimental conditions and using the same probe [5]. The fairly strong temperature dependence evident for the ^{33}S MAS NMR spectra of $NH_4Al(SO_4)_2{\cdot}12H_2O$ and reflected by the C_Q values would immediately suggest that a similar temperature dependence should be observable for C_Q in $KAl(SO_4)_2{\cdot}12H_2O$ because of the general similarities between NH_4^+ and K^+ salts. In this connection we should point out that $NH_4Al(SO_4)_2{\cdot}12H_2O$ and $KAl(SO_4)_2{\cdot}12H_2O$ are both of the α-alums structural type (space group *Pa*3) [15] which includes sulfate ions of high symmetry with the central S atom and one of the oxygens located on a threefold axis. However, single-crystal XRD analysis have indicated structural disorder for the sulfate ions in α-alums, since some of the sulfate groups may have a reversed orientation along the threefold axis [16]. Such a disorder may potentially account for small deviations from axial symmetry for the ^{33}S electric field gradient tensors, i.e., η_Q may deviate slightly from zero.

Because of the larger C_Q (=0.64 MHz) for $KAl(SO_4)_2{\cdot}12H_2O$, determined earlier from the second-order lineshape of the central transition at 17.6 T [2], the question was raised if it would be possible to observe the manifold of ssbs for this alum. However, its ambient temperature ^{33}S MAS NMR spectrum for $\nu_r = 6.0$ kHz in Fig. 4 shows that indeed a very useful ssb spectrum for the ^{33}S satellite transitions can be obtained. Taking advantage of a combination of the 14.1 T second-order lineshape for the central transition and the features/shape for the manifold of ssbs observed for the satellite transitions, we arrive at the opti-

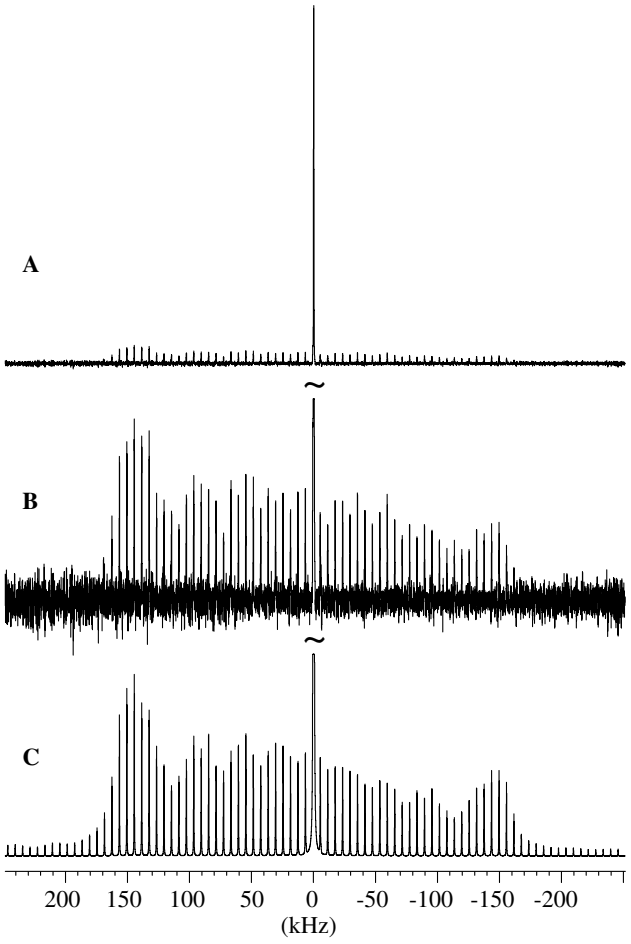

Fig. 4. Experimental and simulated ^{33}S MAS NMR spectra of the satellite transitions for the sulfate ions in $KAl(SO_4)_2{\cdot}12H_2O$. (A) Experimental spectrum acquired at ambient temperature using the 7.5 mm T3 probe for $\nu_r = 6000$ Hz, 295,000 scans with a relaxation delay of 0.5 s, and displayed illustrating the actual relative heights between the central transition and the ssbs for the satellite transitions. (B) Experimental spectrum shown with a vertical expansion larger by a factor 10 than that used in (A) and with a cut-off height of 5.7% for the height of the central transition. (C) Simulated spectrum for the ssbs of the satellite transitions using the (optimized) parameters $C_Q = 638.4$ kHz and $\eta_Q = 0.04$ (Table 1) and a rf offset of 40 kHz (see text) determined from fitting to the experimental ssb spectrum of the satellite transitions.

mized parameters $C_Q = 638$ kHz and $\eta_Q = 0.04$ (Table 1) from the STARS spectral analysis. The simulated spectrum for these transitions, and corresponding to the optimized parameters, is illustrated in Fig. 4C below the experimental spectrum. We should note that the increased intensity of the ssbs to positive frequencies compared to those at negative frequencies relative to the central transition are caused by the use of non-optimized cable lengths either between the probe and the preamp or for the $\lambda/4$ cable in the broadband preamp as pointed out elsewhere [6]. This induces an "apparent" rf offset which can be handled by the STARS simulation/fitting package, as illustrated in Fig. 4C. Although an excellent agreement is observed with the quadrupolar parameters reported recently [2], we again emphasize that the use of ssb manifolds for the satellites usually provides parameters of higher precision (especially for η_Q). Obviously, this advantageous use of the satellite transitions is at the cost of an increasingly larger number of scans required and thus longer spectrometer time. For that reason the VT ^{33}S MAS NMR study on $KAl(SO_4)_2{\cdot}12H_2O$ has been restricted to the observation of the central transition only.

Prior to the start of the VT ^{33}S MAS NMR study on $KAl(SO_4)_2{\cdot}12H_2O$ it was decided to evaluate the effect of slightly different values for the pulse width on the central transition for this compound at ambient temperature (~25 °C) in a similar manner as previously reported in the nutation study by Samoson and Lippmaa [17]. The purpose is to observe the changes in the ^{33}S second-order lineshape and intensity for this transition as a function of an increase in pulse width up to the value of the nominal 90° pulse (τ_p^{90}(liquid) = 5 μs) employed for the 5 mm VT MAS probe. Obviously, this allows determination of the optimum experimental conditions (intensity-wise) and recognition of the second-order lineshapes to be observed in the VT experiments. The experimental spectra showing the intensity and lineshape dependencies for the central transition on the pulse widths of 0.8, 2.0, 4.0, and 5.0 μs are displayed in Figs. 5A–D. These spectra clearly show an intensity dependence on pulse width in accordance with the wellknown relation for a solids 90° pulse [17]

$$\tau_p^{90}\ (\text{solid}) = \tau_p^{90}\ (\text{liquid})(I + 1/2)^{-1}, \qquad (4)$$

i.e., τ_p^{90}(solid) ≈ 2.5 μs for $C_Q \gg \gamma B_1/2\pi$. Just as importantly, the experimental spectra in Figs. 5A–D clearly show a change in the relative intensities for the singularities of the second-order lineshapes. To take full advantage of the observed variation in second-order lineshape and changes in intensities, each of the lineshapes for the experimental spectra in Figs. 5A–D have been individually fitted to simulated spectra using the STARS optimization procedure. The fitting of these spectra employs the "finite pulse" routine of STARS for the pulse excitation, i.e., the density matrix is propagated during the pulse in 5 steps taking the rotational angle of the rotor into account in order to obtain the phase and intensity for each crystallite orientation [18]. Thus, in addition to extraction of the C_Q, η_Q parameters from the individual spectra, the lineshape optimization for each pulse width is also dependent on the employed rf field strength ($\gamma B_1/2\pi$). The four sets of spectral parameters determined from the spectra in Figs. 5A–D are all within the following limits: $\delta_{iso} = 331.7 \pm 0.1$ ppm, $C_Q = 625 \pm 5$ kHz, and $\eta_Q = 0.06 \pm 0.06$. The slightly lower average value obtained for C_Q (=626 kHz) from the 5 mm MAS probe (Fig. 5) compared to the value of $C_Q = 638$ kHz determined from the 7.5 mm T3 MAS probe spectrum in Fig. 4 is most likely caused by a temperature increase of the sample resulting from the increased frictional heating for the 7.5 mm rotor at $\nu_r = 6000$ Hz. The optimized value for the rf field strength $\gamma B_1/2\pi = 47$ (±2) kHz, resulting from the four experimental spectra, is used for all simulated spectra in Figs. 5E–H and is in agreement with

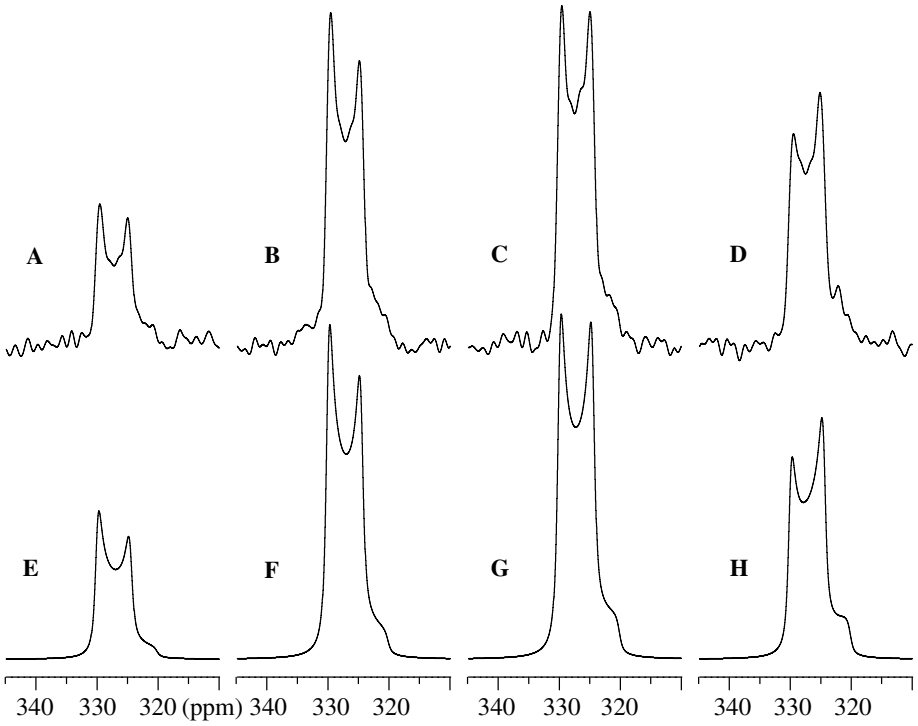

Fig. 5. Experimental (A–D) and simulated (E–H) ^{33}S MAS NMR spectra of the central transition for the sulfate ions in $KAl(SO_4)_2{\cdot}12H_2O$ using a homebuilt 5 mm VT MAS NMR probe for $\nu_r = 10$ kHz and pulse widths of (A and E) 0.8 μs, (B and F) 2.0 μs, (C and G) 4.0 μs, and (D and H) 5.0 μs. The pulse widths employed for the experimental spectra are based on the pulse width calibration for a 1.0 M aqueous solution of Cs_2SO_4 giving τ_p^{90}(liquid) = 5.0 μs or $\gamma B_1/2\pi = 50$ kHz. The STARS optimized parameters determined from the experimental spectra and used in the simulations for all spectra in (E–H) (along with $\nu_r = 10$ kHz, the pulse widths indicated above, and the STARS "finite pulse" routine) are: $\delta_{iso} = 331.7$ ppm, $C_Q = 626$ kHz, $\eta_Q = 0.04$, and $\gamma B_1/2\pi = 47$ kHz (see text).

the value $\gamma B_1/2\pi = 50$ kHz determined from the 1.0 M Cs_2SO_4 solution (see Section 2). The variations in second-order lineshapes and intensities as a function of pulse width/rf field strength, apparent from the spectra in Fig. 5, may serve to be a useful tool in evaluating the optimum experimental conditions when observing the central transition for a quadrupolar nucleus of unknown quadrupole coupling.

Following the information gained from these ambient temperature ^{33}S MAS experiments on the central transition for $KAl(SO_4)_2{\cdot}12H_2O$, a series of five VT ^{33}S MAS spectra covering the range from −46 to +55 °C have been recorded for this transition employing the 5 mm VT MAS probe. With reference to the results shown in Fig. 5, a pulse width of 4 μs for $\gamma B_1/2\pi = 47$ kHz along with a relaxation delay of 0.5 s was used in recording these spectra. The spectral parameters resulting from the STARS iterative fitting ("finite pulse" procedure) of these spectra are summarized in Table 1 along with the corresponding temperatures. These data reveal that the magnitude of C_Q increases with increasing temperature according to the linear correlation shown in Fig. 6. Regression analysis of the data gives

$$C_Q\ (\text{kHz}) = 2.266 \times T(^{\circ}\text{C}) + 555 \qquad (5)$$

with a correlation coefficient $R = 0.9998$. Thus, the temperature dependence for C_Q in $KAl(SO_4)_2{\cdot}12H_2O$ is similar to that observed for $NH_4Al(SO_4)_2{\cdot}12H_2O$, however, with a slightly lower temperature coefficient. From the correlation in Eq. (5) we find that the temperatures of the two $KAl(SO_4)_2{\cdot}12H_2O$ samples corresponding to the "apparent"

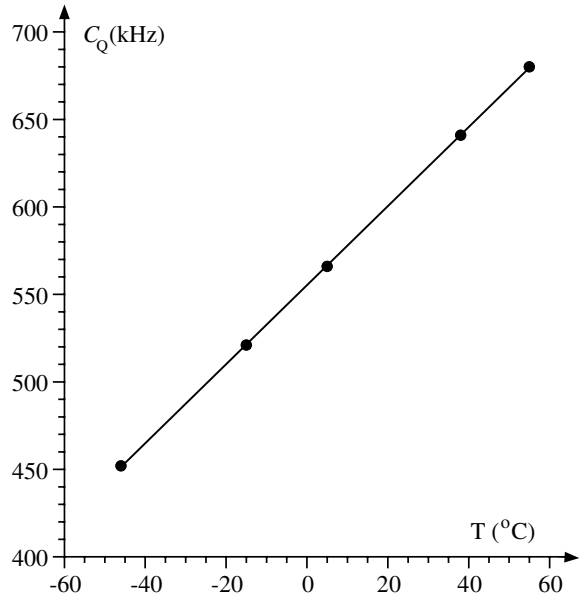

Fig. 6. Regression analysis of the C_Q versus T (°C) data in Table 1 for the temperature dependence of C_Q in $KAl(SO_4)_2{\cdot}12H_2O$. The result shows an excellent linear correlation, expressed by Eq. (5).

ambient temperature spectra in Fig. 4 (7.5 mm T3 probe, $\nu_r = 6000$ Hz, $C_Q = 638.4$ kHz) and Fig. 5 (5 mm home-made probe, $\nu_r = 10{,}000$ Hz, $C_Q = 626$ kHz) are 37 and 31 °C, respectively.

4. Conclusions

Experimental experiences gained from recent improvements in solid-state ^{14}N MAS NMR methodologies [4–10] have been taken into full advantage for its ^{33}S spin-isotope neighbour in the low-frequency end of the NMR-frequency table. Based on this experience, the present study presents the first observation of manifolds of spinning sidebands for the ^{33}S satellite transitions in natural-abundance solid-state ^{33}S MAS NMR as illustrated for the two alums $XAl(SO_4)_2{\cdot}12H_2O$ for $X = NH_4$ and K. For example, precise adjustment of the magic-angle setting (a prerequisite for the observation of decent ssbs) is most conveniently performed by tuning the probe a few megahertz away to its ^{14}N neighbor (without any hardware change to the probe) and using either $(CH_3)_4NI$, $NH_4H_2PO_4$ or $Pb(NO_3)_2$ for the angle adjust [6–8]. The manifolds of ssbs observed for the two alums allow determination of the ^{33}S quadrupole coupling parameters (C_Q, η_Q) with high precision. Acquisition of the ^{33}S MAS NMR spectra at different spinning frequencies indicates a quite large temperature dependence for C_Q. A VT study in the range −35 to 70 °C employing the manifold of ssbs for the NH_4-alum shows a linear temperature dependence and a sign change for C_Q at 4 °C with a temperature coefficient of 3.1 kHz/°C. The changes in intensity and appearance of the second-order lineshape observed for the ^{33}S central transition in the K-alum as a function of pulse width, for a fixed rf field strength of $\gamma B_1/2\pi = 47$ kHz, has been analyzed and an excellent agreement between experiment and theory is observed. The purpose of this analysis has been a determination of the optimum experimental conditions for a VT study of the K-alum employing the central transition, a study which shows a linear temperature dependence for C_Q with a temperature coefficient of 2.3 kHz/°C for this alum. Some interesting applications on the use of ssbs in natural-abundance ^{33}S MAS NMR spectra of the satellite transitions are currently in progress.

Acknowledgments

The use of the facilities at the Instrument Centre for Solid-State NMR Spectroscopy, University of Aarhus, sponsored by the Danish Natural Research Council, the Danish Technical Science Research Council, Teknologistyrelsen, Carlsbergfondet, and Direktør Ib Henriksens Fond, is acknowledged.

References

[1] M. Witanowski, G.A. Webb, (Eds.), Nitrogen NMR, Plenum Press, London/New York, 1973.
[2] T.A. Wagler, W.A. Daunch, M. Panzer, W.J. Youngs, P.L. Rinaldi, Solid-state ^{33}S MAS NMR of inorganic sulfates, J. Magn. Reson. 170 (2004) 336–344.
[3] H. Eckert, J.P. Yesinowski, Sulfur-33 NMR at natural abundance in solids, J. Am. Chem. Soc. 108 (1986) 2140–2146.
[4] H.J. Jakobsen, H. Bildsøe, J. Skibsted, T. Giavani, ^{14}N MAS NMR spectroscopy: the nitrate ion, J. Am. Chem. Soc. 123 (2001) 5098–5099.
[5] T. Giavani, H. Bildsøe, J. Skibsted, H.J. Jakobsen, ^{14}N MAS NMR spectroscopy and quadrupole coupling data in characterization of the IV ↔ III phase transition in ammonium nitrate, J. Phys. Chem. 106 (2002) 3026–3032.
[6] T. Giavani, K. Johannsen, C.J.H. Jacobsen, N. Blom, H. Bildsøe, J. Skibsted, H.J. Jakobsen, Unusual observation of nitrogen chemical shift anisotropies in tetraalkylammonium halides by ^{14}N MAS NMR spectroscopy, Solid State Nucl. Magn. Reson. 24 (2003) 218–235.
[7] T. Giavani, H. Bildsøe, J. Skibsted, H.J. Jakobsen, Determination of nitrogen chemical shift anisotropy from the second-order cross-term in ^{14}N MAS NMR spectroscopy, Chem. Phys. Lett. 377 (2003) 426–432.
[8] T. Giavani, H. Bildsøe, J. Skibsted, H.J. Jakobsen, A solid-state ^{14}N magic-angle spinning NMR study of some amino acids, J. Magn. Reson. 166 (2004) 262–272.
[9] B. Zhou, T. Giavani, H. Bildsøe, J. Skibsted, H.J. Jakobsen, Structure refinement of $CsNO_3$(II) by coupling of ^{14}N MAS NMR experiments with WIEN2k DFT calculations, Chem. Phys. Lett. 402 (2005) 133–137.
[10] E. Fukushima, S.B.W. Roeder, Experimental Pulse NMR, A Nuts and Bolts Approach, Addison-Wesley, Reading, MA, 1981, pp. 407–416 (Tank Circuits).
[11] J. Skibsted, N.C. Nielsen, H. Bildsøe, H.J. Jakobsen, Magnitudes and relative orientation of ^{51}V quadrupole coupling and anisotropic shielding tensors in metavanadates and KV_3O_8 from ^{51}V MAS NMR spectra. ^{23}Na quadrupole coupling parameters for α- and β-$NaVO_3$, J. Am. Chem. Soc. 115 (1993) 7351–7362.
[12] J. Skibsted, H.J. Jakobsen, ^{23}Na MAS NMR of central and satellite transitions in the characterization of the anhydrous, dihydrate, and mixed phases of sodium molybdate and tungstate, Solid State Nucl. Magn. Reson. 3 (1994) 29–38.
[13] STARS is available as part of the VNMR software from Varian Inc. and has been developed and upgraded in our laboratory H.J. Jakobsen, J. Skibsted, H. Bildsøe, N.C. Nielsen, Magic-angle spinning NMR spectra of satellite transitions for quadrupolar nuclei in solids, J. Magn. Reson. 85 (1989) 173–180.
[14] T. Bjorholm, H.J. Jakobsen, ^{31}P MAS NMR of P_4S_3. Crystalline-to-plastic phase transition induced by MAS in a double air-bearing stator, J. Magn. Reson. 84 (1989) 204–211.
[15] H. Lipson, C.A. Beevers, The crystal structure of the alums, Proc. R. Soc. (Lond.) A 148 (1935) 664–667.
[16] A.C. Larson, D.T. Cromer, Refinement of the alum structures. III. X-ray study of the α-alums K, Rb, and $NH_4Al(SO_4)_2{\cdot}12H_2O$, Acta Crystallogr. 22 (1967) 793–800.
[17] A. Samoson, E. Lippmaa, Excitation phenomena and line intensities in high-resolution NMR powder spectra of half-integer quadrupolar nuclei, Phys. Rev. B 28 (1983) 6567–6570.
[18] J. Skibsted, N.C. Nielsen, H. Bildsøe, H.J. Jakobsen, Satellite transitions in MAS NMR spectra of quadrupolar nuclei, J. Magn. Reson. 95 (1991) 88–117.